JURNAL ILMIAH KOMPUTER GRAFIS, Vol.14, No.1, Juli 2021, pp. 150 - 166
p-ISSN : 1979-0414(print)
e-ISSN : 2621-6256 (online)
http://journal.stekom.ac.id/index.php/pixel

ENHANCED NOISE CANCELLATION IMAGE PERFORMANCE USING WEIGHTED AVERAGE (WAV) REPROJECTION

Santi Widiastuti[1] , Ayyub Hamdanu Budi Nurmana Mulyana Slamet[2],
[1,2]Universitas Sains dan Teknologi Komputer Semarang
Email: santi@stekom.ac.id ; ayyub@stekom.ac.id

ARTICLE INFO

Article history:

Received 19 Maret 2021
Received in revised form 17 April 2021
Accepted Juni 2021
Available online 23 Juli 2021

ABSTRACT

Main Objective: This research targets AP sizing entrenched on image structure to raise denoising performance using an improved method for classifying image pixels. Background problem: Digital images may be blended by noise while the addition or communication process, affecting the authentic image signal. Image noise can cause problems at several stages of image processing equally image distribution. Accordingly, image denoising is a significant activity to recover the initial clean image signal from the detected noise signal. Novelty: The proposed WAV method has been refined and improved regarding the classification scheme, and the APS, and the classification results can be used as a mask on the noise image to fix identical patches. Research Method: This study proposes a WAV reprojection algorithm, with the PS being set dynamically entrenched on the image structure. Image structures are consistently taken with an upgraded and enhanced analysis method entrenched in the structure tensor matrix. Analysis results are also used to develop the analysis of comparable patches in images. Finding/Result: Empirical outcomes present that the noise cancellation work of the suggested method is better than the authentic WAVRA, along with several other modifications of the NLMA. Conclusion: In intensity profiles, the proposed method mostly has fewer changes to the original image values than other methods, thus, this method can be continued again to color images, and can also be applied to various types of data such as medical images.

Keywords*: Weighted Average (WAV), Noise Cancellation Image, Non-Local Means (NLM), Adaptive Patch*

Received Maret 19, 2021; Revised Juni 17, 2021; Accepted Juli 21, 2021

JURNAL ILMIAH KOMPUTER GRAFIS p-ISSN : 1979-0414 e-ISSN : 2621-6256.

1. Introduction

Several picture-denoising approaches have been proposed in several previous studies, but most of the results achieved are only denoising in an average way that can be done in the spatial domain such as the "Gaussian Smoothing" model (Hostettler et al., (2019), "Anisotropic Filtering (AF))" (João et al., (2020); Qian et al., (2022), and "minimization of Total Variation" (Rudin et al., (1994); or in the frequency domain such as the "Wavelet Thresholding" method (Akkar et al. al., (2019); Umoh et al., (2020); Portilla et al., (2003) " Patch-Based Denoising Algorithm" (PBDA) has devoted more than consideration in the area of noise canceling image, where neighboring patches in a particular hunt window joining in the noise canceling progress for a particular hint plot in a noise image. This support the best approximation for the initial picture signal from its noise signal.

PBDA is popular in the field of image denoising, and it makes use of in-image similarity, in which the image signal is recovered by averaging among identical patches in the image. The latest research proposed PBA "Non-Local Means" or "NLM" for noise-canceling images. A variant of the "NLMA" (Algorithm) is suggested to develop its work by dynamically choosing some internal parameters. Some of these variations have defined abrading parameters dynamically based on image structure (Verma, (2018); Ceng, (2017) or based on noise levels (Zhu et al., (2014). Several other types are based on "adaptive patch size" (APS) selection using image structures (Hu, (2013); Lan, (2013). In addition to APS, Charles et al., (2012) suggested a form of an AP to overcome the issues of "halo noise" in the edges. Several variations have developed the NLMA by developing the computational approach to the connection between patches (Lin et al., (2020); Peter et al., (2012); Wu et al., (2014).

Another important development in patch-based noise canceling methods is the "WAV reprojection algorithm" (WAVR) (Salmon et al., (2012) which moves the reprojection mechanism from the plot area to the pixel area. The WAVR used improvement of the entire patch, in which all pixels in the patch are overburdened to improve denoising work. Whatever the image structure, the main parameters of the WAVR remain constant. The focus of this research is to develop the work of the WAVR by setting an APS entrenched in the image structure. In addition, this study also proposes to develop the WAVR by improving patch identity.

"Edges are better preserved with small patch sizes while smooth regions have better denoising performance with large patch sizes" (Zeng et al., (2017). In the WAVR, the PS has been tuned to solve the disregarding of the image structure. Thus, an APS WAVR based on image structure is proposed in this study. Image pixels are restricted based on an enhanced analysis method. In this study, Zeng et al., (2011) classification method is based on the eigenvalues of the texture tensor matrix. The approach is obtained by mixing it with a disruption index (Zeng et al., (2017) which classifies image pixels into three regions. In addition, a pre-processing procedure is taken to the image that has noise to decrease the total noise that affects the analysis procedure. Pixels Images are restricted into three classes: smooth, edge, and textures/noises. The analysis results will later be taken as a mask on a noise image to dynamically determine the PS. In addition, the classification scheme is also used to develop the search method for identical patches because two patches are considered identical when coming from the same class. The suggested method has developed the authentic WAVR in terms of PS-NR and MSS-IM work and has better edges and textures in the images..

p-ISSN : 1979-0414 e-ISSN : 2621-6256

2. LITERATURE REVIEW AND HYPOTHESIS DEVELOPMENT

Digital images are generally troubled by rejected signals (noise) while the recovery process. Image noise can impact some issues in image processing further recognition, and distribution. Noise become in various styles. Each method is taken to stem different noise structures.

AWGN

AWGN or "Additive-White-Gaussian-Noise" is mostly general noise treated in image processing. Dynamically noise appears in a noise sign and all are joined to the authentic image signal with an(i) = b(i) + c(i), where a is a noise image, b is a clean image, and c is noise. In AWGN, noise has a constant strength at all densities with the magnitude ensuing a Gaussian circulation.

$$(d) = \frac{1}{\sqrt{\pi\sigma^{\theta}}}^{\frac{(d-\pi)^2}{2\sigma^2}}$$

2.1 Noise Level Estimation

Some approaches for estimating various noises are commonly restricted and entrenched on filters, patches, and statistics. The filter-based approach estimates noise with a pre-dribble movement adopting a low pass dribble to censor image structure (Kumari, (2017); May, (2022). Then, noise is predicted as the variation between the purified image and noise. Patch-based noise prediction describes the image into patches. Then, homogeneous patches are adopted to predict the noise level. The key problem in the patch-based approach is how to determine homogeneous patches. In addition, some methods are based on the patch and require a high computational load because this method estimates noise iteratively. The statistical method analyzes the distribution of local variance. The results are stronger because the statistical method used is not sensitive to outliers (Ghazal et al., (2011). This study will only be limited to determining the noise range (low, or high) so this study uses filter-based noise level prediction is just an easy method that does not lack a high computational load.

2.2 Statistically Based Noise Estimation

Local variance distribution analysis was taken to predict noise in a statistical-based method (Fernandez et al., (2009). Some image is ravaged into several pieces with small size, and from each block, the local intensity fluctuation is determined. The fluctuation of all pieces is moderate to predicted noise types because the size of the beam taken must be as small as possible.

Image Denoising

In the dimensional sphere, spatially neighboring pixels are treated in noise canceling, equally Gaussian kernel involution. In the regularity domain, the pict is updated to the regularity sphere such as the "Fourier transform" or the "Wavelet transform" (Othman et al., (2020). Filtering is carried out in the frequency domain, then the reverse transformation is applied to obtain a denoise image. Recently, PBDAs have become very familiar in the noise cancel area, and take dominance of the affinity in pict. Thus, calculating is accomplished entrenched on the affinity between image patches. Xu et al., (2020) refined the NLMA in another patch-based noise-canceling algorithm, that has the best work output in noise canceling is "BM-3D" (Hasan et al., (2018).

2.3 PBDA

"Patch-Based Denoising Algorithm" or shorted in PBDA is essential for landscape images to have a high level of affinity, meaning that different small pieces have many identical pieces in the same picture. The PBDA returns the image signal by fraudulent in this affinity.

2.4 NLM Algorithm (NLMA)

NLMA measures the authentic image signal by seeing the neighboring areas of the currently refined pixel. All pixels find all identical patches around the image that test the patches over the currently refined pixel. Similar patches are selected in multiple situations entrenched on affinity in gray level values, geometric composition across neighborhoods, and the range of the previous pixel. Formerly, an intact moderate of all the centered pixels across all identical patches is determined. The weight depends on the affinity between patches. That is, pixels whose environment is identical in gray level values to the currently refined pixels have more weight than another pixel, and nearby pixels have more density than far pixels. Yang et al., (2013) suggested an approach for selecting smoothing parameters dynamically. In here, the smoothing parameter is determined entrenched on the limited gray various level of the image pixels. Variation of the limited gray level analyzes the format of the image, characterizing between noise and the edges of the image. Limited gray level variations are determined by:

$$\sigma_l^2(x,y) = \frac{1}{Z^2-1} \sum_{i,j=\frac{-(D-1)}{2}}^{\frac{Z-1}{2}} [I(x+i,x+j) - p_l(x,y)]^2$$

This is entrenched on the resulting analysis, limited smoothing parameters are defined to pixels on the edges and extensive smoothing parameters are defined to pixels in a smooth field. Verma et al., (2018), proposed another method for dynamically selecting smoothing parameters. In this method the image area is classified using Gray's relative investigation, which is related to the gray system theory (Deng, (1982). Gray's relative investigation is tested when some information is lost. It treasures a trove of the relationship between one factor and all other factors in a system. Values of the gray relationship between image patches were determined by adopting Gray's relative investigation. Formerly, dimensional smoothing parameters were defined to different pixels entrenched in the resulting analysis.

Another method for setting adaptive smoothing parameters is based on discontinuity indicators (Zeng et al., (2017). A new gap index is suggested to catch the image format. “The gap index is imitative from the eigen values of the tensor structure matrix” (Knutsson, (1989). It is captured as the variation between the 2 eigen values for the different pixels. The resulting gap index is adopted to identify image pixels. If the discontinuity index is bigger, then the pixel is treated to be on the edge. If it is not big and both eigenvalues are also small, the pixel is considered to be in the smooth area. A pixel is a noise if the gap index is not big and both eigen values are bigger. Therefore, the flexible smoothing parameter is selected for different pixels entrenched in the resulting analysis. Liu et al., (2012) suggested increasing NLM by adopting the NLM approach for 2nd time. 1st is the variation of noise predicted by adopting a weakly structured noise patch estimate. Weakly structured patches are chosen and entrenched on the image grade. Then, “Principal Component-Analysis” or “PCA” is tested on the chosen patches to access an assessment of the noise level. Then, the Non-Limited mean method is tested to the noise image by using dimensional smoothing parameters entrenched on the predicted various noise to obtain the elemental prediction. The eventual prediction is then captured by taking the Non-Limited approach with less smoothing.

Dimensional NLM uses Weight Thresholding

Asif et al., (2016) proposed NLM to use "Weight Thresholding". The essential assessment is stemming in the 1st step by creating a threshold pixel weight in the search field. All densities raised to the brink value do not change, but the density that is no more than the brink value is set to 0, so those pixels are deleted from the density average action. Formerly, in 2nd step, the density threshold NLM was taken again but in various smoothing strengths. The brink value is set adaptively entrenched on the noise level.

p-ISSN : 1979-0414 e-ISSN : 2621-6256

2.5 APS NLM

APS (Adaptive-patch-size) on image texture

"Patch sizes" (PS) have been fixed to be established in the authentic NLMA. Adopting the PS variable has an important increase in the work of the NLM approach. Edges are better dry with not big PS during smooth planes and have got good noise canceling work than with bigger PS. Different APS NLM denoise algorithms are suggested to affect the ineffectiveness of conventional NLM. Lu et al., (2014) suggested an APS NLMA, which uses a tensor structure to classify images into fine areas and textures. The characteristic of the 2 tensor eigen values of the texture is measured. If the characteristic of the 2 eigen values is big so the pixel is treated to be in a smooth field and a bigger PS is assigned to approximate the authentic value. Furthermore, if the characteristic is not big then the pixels are treated to be in the texture field and thus a not-big PS is added to approximate the authentic value. Luo et al., (2017) have also developed the NLMA by selecting PS dynamically based on image structure, with local image geometry and noise deviation to push present metrics,

$$R(i) = f(i)\left(\frac{\lambda 1_1^2 - \lambda_2^2}{\lambda 1_1^2 + \lambda_2^2}\right)$$

λ1 and λ2 are the eigen values of the texture tensor adopted to identify the image texture. This array metric identified images into 4 areas (c1, c2, c3, and c4) following their correlation to the 3 crate values T1, T2 and T3 is ninety, seventy and thirty percent,

$$i\epsilon \begin{cases} c_1 & R(i) \geq T_1 \\ c_2 & T_2 < R(i) < T_1 \\ c_3 & T_3 > R(i) \leq T_2 \\ c_4 & R(i) \leq T_3 \end{cases}$$

c1 produce a textured area with a not big noise divergence value, c2 is an intermediate are that has a smaller noise divergence and no more texture, c4 is an empty area, and c3 produces an area with a textured and big noise value. So, different PS is added into different areas. The biggest PS is defined to the empty field c4, and the other PS is defined to c3 because it has more texture. The PS boosts constantly in c1 and c2 because those areas have no more structure. Xia et al., (2013) suggested an APS NLM method entrenched on homogeneity area, with the PS and search window size set adaptively providing on the limited extent size, this finds a homogeneous area in the image alike to the image texture (Saha et al., (2000). The range of homogeneity is large within the region and becomes smaller at the edges. Therefore, the local scale is calculated for different pixels, and the PS search window size is set appropriately.

NLM AP Forms

In addition to APS, Charles et al., (2012) suggested a form of AP to overcome the issues of "halo noise" in the edges environment. Various shapes have been used including square, disc, pie, wedge, and ribbon. Shape variations are applied to deal with the geometric texture of the image. "Fast Fourier Transform" is taken to handle various forms of patches.

PS and Noise Variant

Knowledge of the noise variance improves the performance of the NLMA. The PS is also damaged by the noise deviation. With a big noise deviation, the use of larger patches has good than noise-canceling output (Duval et al., (2011)). So, it is better to use a large PS for noise resistance. Furthermore, deciding on a bigger PS avoids result common ground for small minutiae, and decreases denoising work in the edges environment. Therefore, the authors suggest selecting a dimension smoothing parameter for the comprehensive PS to affect the edge smoothing problem.

NLM with Enhanced Similarity Computational Methods

The "Euclidean" area from the geometric image texture is adopted to treasure trove identical patches. This approach is entrenched only in noisy images, which may not efficiently bring structural affinity, especially with high noise deviation.

NLM-based K-Means Clustering

"K-means clustering is mixing with the NLMA to develop similar patch matching" (Peter et al., (2012). "The K-Means algorithm allocates image pixels into a total of clusters entrenched on their intensity area from the centroid" (Hartigan et al., (1979). "The noisy image is smoothed using a Gaussian smoothing filter Gaussian filtering" (Naik et al., (2022) recover the image signal by applying a Gaussian kernel convolution to an I0 noise image.

$$I_m = \sum_{i=1}^{K} \sum_{x_j \in S_i} ||x_j - \mu_i||^2$$

Im generated image is used as a mask for the noised image to develop similar patch identical. Finally, the denoized image is obtained as a entire moderate of pixels in the same neighborhood Ω in cluster n as follows:

$$NL[v_n](i) = \sum_{j \in \Omega} w(i,j) v_n(i)$$

DCT based NLM

To increase patch affinity, the dimensional area between patches is changed with the area "discrete-cosine-transform" or "DCT" coefficients (Yakut, (2021) in the "frequency domain" (Lin et al., (2020). Neighboring plots are changed from the dimensional sphere to the "DCT" density sphere. Moreover, the "DCT coefficients" are captured in Zig-zag scanning. As a result, the weights in the NLM mechanism are recovered by:

$$w(i,j) = \frac{1}{Z(i)} e^{-\sum_{k=1}^{d} \frac{(C_d(N_i)_k - C_d(N_j)_k)^2}{h^2}}$$

2.6 WAVRA

The WAVRA has important improvements in the patch-based denoising method. The WAVRA (Salmon et al., (2012) has developed the method of reprojecting from patch area to pixel area. Denoising is carried out in 3 ways: getting identical patches, denoising different patches, and reprojecting patches that are denoised to the pixel sphere.

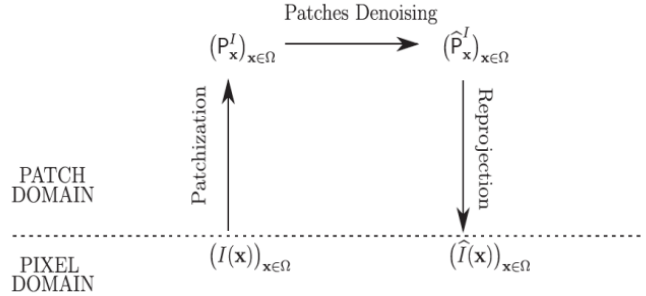

Figure 1. The 3 ways of WAVRA (Salmon et al., (2012)

In the first step, the chi-square distribution of $\chi 2$ together with the "Euclidean" area is adopted to analyze the similarities in the patches. 2 patches are treated identically if the "Euclidean" area is no more than the $\chi 2$(W2). To measure pixel over the clustering ways, the intact moderate of each x guessor across all patches that belong to pixel x is measured.

p-ISSN : 1979-0414 e-ISSN : 2621-6256

$$I_{W_{av}}(x,y) = -\sum_{i=1}^{W^2} \beta_i P_i (W^2 - i + 1)$$

The βi weights are entrenched on degrading the deviation in patches. Therefore, the WAVRA adds the empty kernel, βi is comparable to the total of adopted to evaluation ⟦ P⟧ _iand ∑_(i=1)^(W^2)⁡ ⟦β_i=1⟧ . The WAVRA takes dominance of the entire patch, that is, all pixels in a plot are overburdened, which improves noise cancellation work. The NLMA is completely low in the edge environment due to the edge-centered patches having multiple plots that are identical. Decentralized patches are taken in the WAVRA to improve noise cancellation work in the edge environment. The decentralized patch has a patch that is more similar to the patch in the middle, especially around the edges taking dominance of the entire patch, that is, all the pixels in the patch are overburdened, which improves denoising performance. The NLMA works lowly in the edges environment because edge-centered patches have multiple plots that are identical.

Decentralized patches are added in the WAVRA to improve noise cancellation performance around the edges. A decentralized patch has more identical patches than the patch in the middle, especially around the frame (edge). The WAVRA grant for more fast application for 2 criteria. 1st is to use an empty kernel rather than a "Gaussian Kernel". With an empty kernel, all entries have the same density during Gaussian is fitting more estimate as the density alters from entries to the candidate. Empty kernels have dominance also in noise cancellation work, it decreases the issue endured by the "Gaussian kernel" in the NLMA when the search window is mostly big. Entries are more weighted, and this influence the effect of great entries. The empty kernel strengthens the guesser with a small hard brinking coefficient. 2nd reason is associated with the size of the search window, the WAVRA has good results with small search window sizes, for example (search window = 9). The zone of influence is wider because the patch is decentralized. The zone of influence in the middle patch with search window R and PS W is R + W − 1. Nonetheless, the decentralized patch has a wider zone of influence, which is R + 2W − 2.

Image denoising with BM-3D

BM-3D (Hasan et al., (2018) consists of two screening steps; hard thresholding screening (Umoh et al., (2020) which provides basic estimates, and Wiener screening (Robinson et al., (1967)) which produces final estimates. The different processes consist of 3 actions: clustering, combining filtering, and gathering. Different asset pieces are measured with other pieces in the image on clustering action. Euclidean distances are analyzed, and identical pieces are selected if their area is no more than a stated brink.

$$S_{xR} = \{x \in X | d(Z_{xR}, Z_x) < \tau match\}$$

All the matched SxR blocks are deformed to shape a 3D ZS xR array. The 3D transformation τ3D tested into the ZSxR 3D array to build a meager image. Strong brink is tested into the transformation coefficients, with results in various evaluations for different pixels because the evaluation may overhang. Furthermore, the different estimator has accustomed a density that is contra comparable to the total of non-0 coefficients. In the gathering action, the density moderate of all evaluations is measured to arrive at an essential image measure. In the 2nd processing action, "Weiner filtering" is taken into the local stacked Y^SxR estimates resulting from the hard brink action, and the deformed match pieces from the noised imagery. Then, the density moderate is measured to get the end measure of the image. Although BM-3D has a competent enhancement of the patch-based noise cancellation domain, it is more time-consuming because it commits 2 renewal actions.

BM-3D uses Adaptive Thresholding

To develop the thresholding action, "adaptive hard-thresholding (AHD) is carried out as stated in the hard thresholding step in the BM-3D Method" (Alkinani et al., (2017). AHD is

chosen to entrench the similarity of geometric distances and lighting between patches. More thresholding is defined to the patch transformation coefficient if a patch is geometrically unclosed from the assets patch. The mixing "Weiner filtering" action is also developed by defining more density to identical patches. The density here is used for the 3D array patches. More weight is defined to identical patches. PS-NR is adopted as a patch affinity in choosing the weight.

3. METHODOLOGY

The WAVRA is the most capable patch-based noise cancellation algorithm. This is an easy and efficient approach to noise canceling in the dimensional sphere. In contrast to the NLMA, all pixels in a patch are overburdened in the WAVRA. The tight PS is adopted in the noise-canceling action. The affinity between patches is measured using the "Euclidean area" between patches. In this study, the PS was determined actively entrenched in the image texture. The image structure is classified using a tensor structure matrix. It classifies image pixels into 3 classifications. Moreover, the analysis output is adopted to develop the combining of identical patches. Patches that are identical to the assets patch devote to the averaging action if their center pixels are of the same classification.

3.1 Enhanced WAVRA

Prior knowledge of drawing structures supports setting parameters correctly. Frame information is better retained with not big PSs, during smooth planes have better noise cancellation work with bigger PSs. In the WAVRA, PS is set to be fixed disregarding the image texture. This study targets APS adjustment based on image texture to improve the work of noise cancellation image and the image pixels need to be restricted first. An improved method is taken to identify image pixels.

3.2 Enhanced Classification Methods

"Image pixels were first analyzed using the eigen values of the texture tensor matrix" (Knutsson, (1989). The texture tensor matrix is described as:

$$T_\sigma = \begin{bmatrix} j_{11} & j_{12} \\ j_{21} & j_{22} \end{bmatrix} = \begin{bmatrix} G_\sigma * (g_x(i,j))^2 & G_\sigma * g_x(i,j)(g_y(i,j) \\ G_\sigma * g_y(i,j)g_x(i,j) & G_\sigma * (g_y(i,j))^2 \end{bmatrix}$$

Then, the two eigenvalues are calculated:

$$\lambda_1 = \frac{1}{2}(j_{11} + j_{22} + \sqrt{(j_{11} + j_{22})^2 + 4j_{12}^2}$$

$$\lambda_2 = \frac{1}{2}(j_{11} + j_{22} + \sqrt{(j_{11} + j_{22})^2 + 4j_{12}^2}$$

Where $j_{11} = G_\sigma * (g_x(i,j))^2$, $j_{22} = G_\sigma * (g_y(i,j))^2$and $j_{12} = G_\sigma * g_x(i,j)(g_y(i,j)$. The complete contrast between the 2 eigen values λ1 and λ2 is then determined:

$$\lambda = |\lambda_1 - \lambda_2|$$

Ensuing the analysis structure is adopted to identify image pixels:

$$(i,j)\epsilon \begin{cases} c_1 & \lambda(i,j) \le \lambda_2 \dfrac{(\lambda_1 - \lambda_2)}{n} \\ c_2 & \lambda(i,j) \le \lambda_2 \dfrac{(\lambda_1 - \lambda_2)}{n} \\ & \cdots \\ c_n & \lambda(i,j) \le \lambda_n \dfrac{(\lambda_1 - \lambda_2)}{n} \end{cases}$$

p-ISSN : 1979-0414 e-ISSN : 2621-6256

This classification is not accurate, because some pixels may have more than 1 group. In addition, it fall to identify image pixels at a high noise level where the red color represents frame pixels, the blue color represents smooth pixels, and the green color represents texture/noise pixels. In the noise σ = 40, it can be seen that the stated mechanism falls to describe the image texture. Thus, improving the classification in the above equation is proposed by mixing it with the gap index by Zeng, (2017). The gap index classifies image pixels into smooth, frame, and noise. If λ(i, j) is not small the pixel is treated to be on the frame. If λ(i, j) is not big and the 2 eigen values are also not big, then the pixel is treated to be in a smooth area. A pixel is a noise if λ(i, j) is not big but both eigen values are not small. In this study, image pixels are classified into three classes based on comparisons made based on the 2 eigen values of the texture tensor matrix. The 2 eigen values of the different pixels in different classes resulting from the previous Eq are compared with the stated brink values. If both eigen values are no more big than the brink then the pixel is treated to be in a smooth region. If the maximum eigen value λ1 is greater than the brink and the minimum eigen value λ2 is less than the threshold, then the pixel is considered an edge. Pixels are in noise if both eigen values are greater than the brink.

$$(i,j) \in \begin{cases} Smooth & \lambda_1 < \tau, \lambda_2 < \tau \\ Edge & \lambda_1 > \tau, \lambda_2 < \tau \\ Texture\ or\ Noise & \lambda_1 > \tau, \lambda_2 > \tau \end{cases}$$

Moreover, preprocessing steps are also carried out to improve the classification results. Images are denoized 1st is taking the authentic WAVRA. This process has developed the analysis results, especially at low noise levels. The textured area can be restricted as the third class when the noise level is no more than thirty. Nonetheless, if the noise level is high so the 3rd group will produce noise. In addition, the proposed analysis method has orderly the image texture even though the noise level is high. Analysis outputs are given in each noise level (σ = 10, 40, 70, and 100). The smooth area (blue), the edge (red), and the noise area (green). When the noise level is low (σ = 10), the green color only shows the texture. Texture and noise are presented in green when the noise level is high (σ = 40, 70, and 100). With increasing noise, texture pixels tend to be presented as smooth pixels because the texture areas become blurry as a result of the noise cancellation process. Nevertheless, the proposed approach has orderly the frame despite the high noise level. The developed analysis method has better output. The noise signal can be great from the authentic image signal, whereas in the mechanism the areas are restricted as low noise textures.

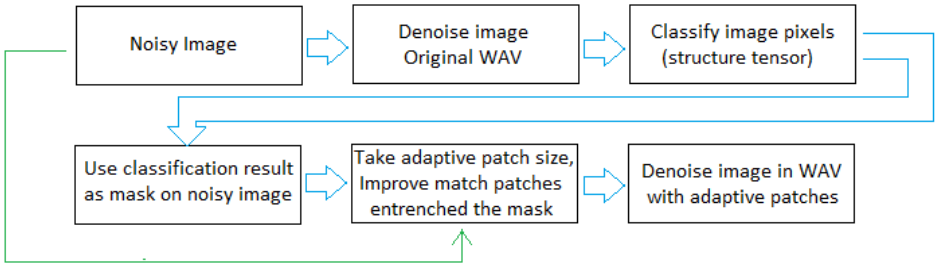

Figure 2 – The basic steps of the improved method in this study

Enhanced WAV Reprojection Method

Fig 2 shows the chart of the scheme suggested in this study. After the analysis stage, this study continues to use the resulting analysis as a mask for a noisy image. The developed mechanism is then collected as follows: In the patching action, patches that are identical to the hint patch grant to the mapping process only if their center pixels belong to the same class. That subtracts the total of dissimilar patches from the average in-process contribution. Moreover, an APS is assigned to each pixel based on that pixel class. The large PS is assigned to the pixels on

the smooth area, and the small f is defined to the pixels on the edge. For textures, a smaller PS is set.

4. EXPERIMENTAL RESULTS

4.1 Noise image generation

An AWGN signal is combined with the authentic image signal to noise image. In this experiment, a noise v image is generated from a clear image u adopting the ensuing equalization in the "Matlab command v=u+sigmaxrandn (size(u))". Peak signal-to-noise-ratio (PS-NR) and "Mean Structure Similarity Index" (MSS-IM) are used to compare the denoising work of the suggested approach with another actual approach in the noise cancellation area. It is the most essential equitable measure of image-denoising algorithm performance. Other subjective comparisons were also carried out in this study, in addition to the visual aspect and strength portrait of the proposed mechanism compared to another ambitious approach.

4.2 PS-NR

PS-NR (Peak Signal to Noise Ratio) is the proportion between the top capacity of the authentic signal and the noise that affects its aspect. PS-NR is detailed through MSE (Mean-Squared-Error) which is determined as the variation between the authentic image u and the depraved image v.

$$MSE = \frac{1}{PxO}\sum_{i=1}^{P}\sum_{j=1}^{O}(v_{ij} - u_{ij})^2$$

where P and O are the image dimensions. Then, the PS-NR is determined as:

$$PSNR = 10log_0\left(\frac{(MAX)^2}{MSE}\right)$$

4.3 MSS-IM

MSS-IM is the contrast in perception between 2 images. It has an convenience more than PS-NR in that it deals with similarities between different patches in the image and not just pixel by pixel. MSS-IM between 2 patches:

$$SSIM = \frac{(2\mu_x\mu_y + c_1)(2\sigma_{xy} + c_2)}{(\mu_x^2 + \mu_y^2 + c_1)(\sigma_x^2 + \sigma_y^2 + c_2)}$$

where μx is the average of x, μy is the average of y. The bigger value express a better result of noise canceling, which is regular over all MSS-IMs, this adopted a measure of the aspect of noise canceling work.

5. RESULT

5.1 Performance Analysis using PS-NR

The average PS-NR value of ten images is serve by configure 3 and the PS-NR value is the resolution at different noise levels for the different algorithms. The value in bold indicates the best PS-NR performance. Fig 3 analyze the regular PS-NR between the suggested mechanism and other noise-canceling image texture. The output shows that the suggested mechanism surpasses the other approach when the noise level is no more than ninety. The average PS-NR value at all noise levels has great results with the suggested mechanism. The PS-NR values of the Window images are also served in Table 2, it serves the PS-NR work in ten various noise levels for the different algorithms. Fig 4 shows a PS-NR comparison between the suggested approach and other

p-ISSN : 1979-0414 e-ISSN : 2621-6256

noise cancellation image approach on Window images. The output is show that the suggested mechanism has the best PS-NR work when the noise level is over twenty.

Table 1 – Average PS-NR values

Noise level	NLM	WAV	Adaptive shape NLM	Proposed method
10	33.28	33.41	33.89	**33.93**
20	29.67	30.31	30.41	**30.45**
30	27.50	28.20	28.19	**28.30**
40	26.02	26.61	26.57	**26.82**
50	24.93	25.43	25.39	**25.65**
60	24.08	24.54	24.52	**24.76**
70	23.40	23.85	23.86	**24.07**
80	22.84	23.30	23.33	**23.49**
90	22.35	22.84	22.89	**22.97**
100	21.93	22.42	**22.51**	22.50
Mean	25.60	26.09	26.16	**26.29**

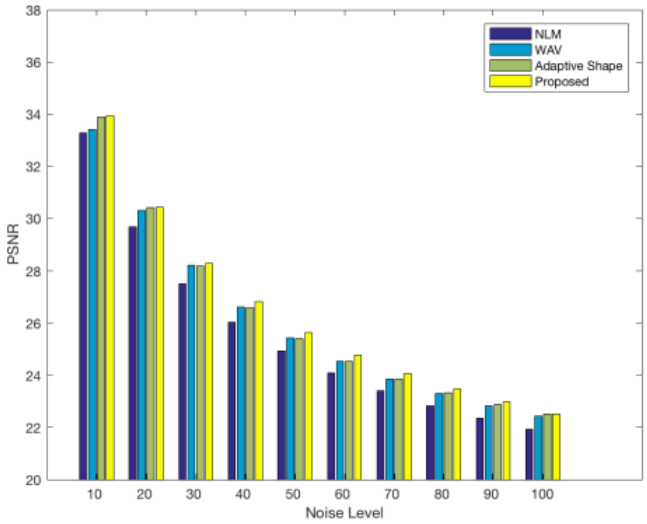

Figure 3 – The average PS-NR value

Table 2 – PS-NR values of Window

Noise level	NLM	WAV	Adaptive shape NLM	Proposed method
10	34.94	34.93	**35.69**	35.39
20	30.82	31.28	**31.69**	31.49
30	28.20	28.87	28.91	**29.09**
40	26.47	26.98	26.79	**27.26**
50	25.28	25.60	25.38	**25.96**
60	24.42	24.66	24.48	**25.05**
70	23.75	23.99	23.86	**24.37**
80	23.21	23.49	23.39	**23.81**
90	22.75	23.07	23.00	**23.32**
100	22.35	22.69	22.66	**22.86**
Mean	26.22	26.56	26.58	**26.82**

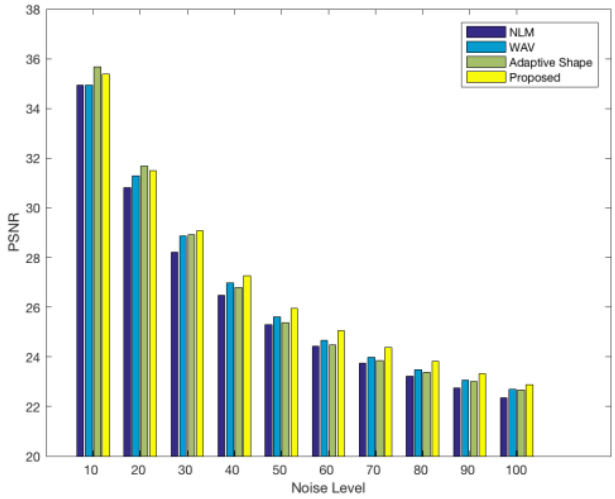

Figure 4 – PS-NR values from Window images

5.2 Work Analysis using MSS-IM

The work of the suggested mechanism is correlated phrases of MSS-IM with different noise cancellation structures. The MSS-IM values generated from ten image sets are shown in table 3. Figure 5 compares the MSS-IM values of the suggested mechanism and different noise-canceling schemes. If the level of noise is no more than seventy so the proposed approach has the best MSS-IM work. The AP sphere has the greatest output when the noise level is high. The average overall noise levels show that the suggested mechanism has the best output. The MSS-IM work of the Window images is also served in Table 4, where the suggested mechanism has the greatest MSS-IM output when the noise level is over than twenty. Fig 6 shows a comparison of the MSS-IM of the suggested method and other denoising methods.

Table 3 – Average MSS-IM values

Noise level	NLM	WAV	Adaptive shape NLM	Proposed method
10	0.950	0.961	0.959	**0.962**
20	0.888	0.904	0.901	**0.906**
30	0.830	0.845	0.845	**0.850**
40	0.780	0.789	0.792	**0.799**
50	0.736	0.737	0.744	**0.750**
60	0.697	0.691	0.702	**0.706**
70	0.662	0.649	0.666	**0.668**
80	0.630	0.613	**0.634**	0.632
90	0.601	0.580	**0.604**	0.597
100	0.575	0.550	**0.578**	0.563
Mean	0.735	0.732	0.742	**0.743**

p-ISSN : 1979-0414 e-ISSN : 2621-6256

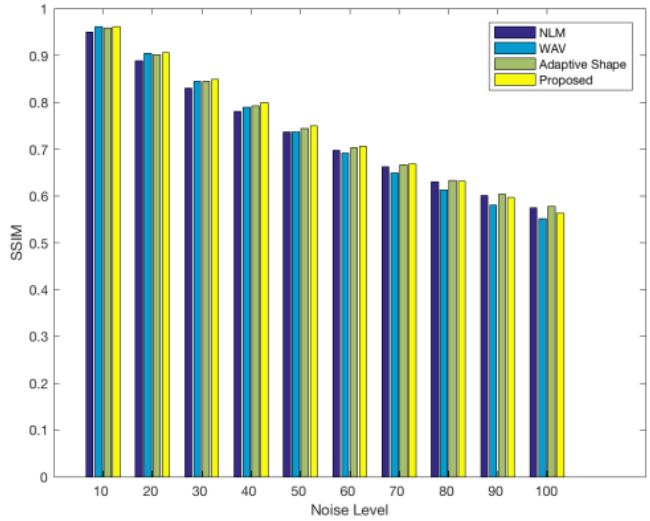

Figure 5 – MSS-IM average value

Table 4 – MSS-IM values of Window images

Noise level	NLM	WAV	Adaptive shape NLM	Proposed method
10	0.971	0.974	**0.975**	0.974
20	0.922	0.929	**0.931**	0.930
30	0.864	0.874	0.875	**0.880**
40	0.807	0.815	0.811	**0.825**
50	0.755	0.755	0.750	**0.771**
60	0.709	0.700	0.699	**0.723**
70	0.670	0.653	0.657	**0.679**
80	0.635	0.614	0.622	**0.638**
90	0.604	0.579	0.590	**0.601**
100	0.576	0.548	0.562	**0.564**
Mean	0.751	0.744	0.747	**0.758**

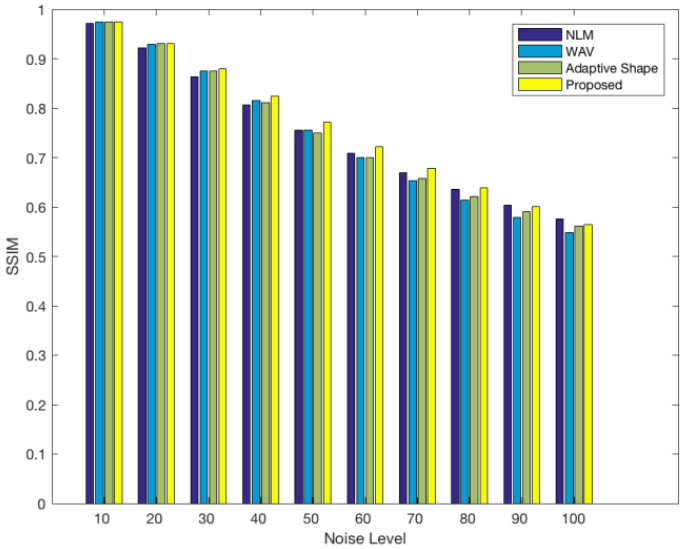

Figure 6 – MSS-IM value of the Window image

5.3 Comparison of Visual Aspect

It is significant to judge the visual aspect of the denoized image. The visual aspect of the suggested mechanism is related to other noise-canceling algorithms. Comparison of visual in the Window images when the noise is σ = 10, 30, 50, and 70. The suggested mechanism and the AP sphere approach are better noise attenuation of the area of interest when the noise level is ten,

whereas the reprojection algorithm WAV and NLMA generate artifacts in the same field of interest. At noise σ = 50, and 70, the zoomed part shows that the suggested method better preserves the frame of the window cage field and the structure centrals the window, for the method has a more fuzzy frame.

5.4 Identification Adopting Intensity Profiles (IP)

The IP on the Window image is adopted to measure the work of the proposed algorithm with another approach, using 2 varieties of horizontal lines. Larger values indicate a large innovation in the authentic picture signal, and small values indicate little change in the authentic picture signal. To analyze the work of the suggested mechanism with another approach, the differences resulting from the proposed method are plotted with each method. Methods are presented in red, while other competitive methods are presented in blue. The suggested method has fewer errors than the authentic WAVRA and adaptive patch shape in most cases.

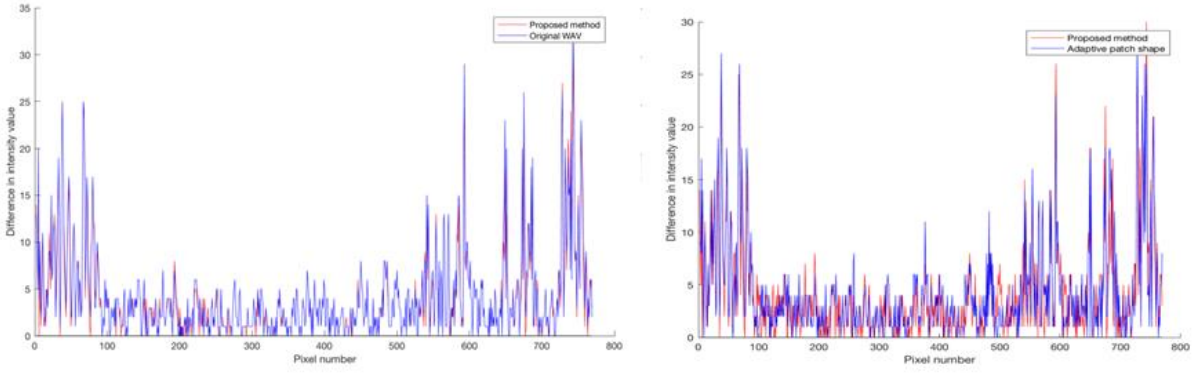

Figure 7. (A) Differences in intensity profiles when the WAVRA and the suggested method are applied along the line y = 450. (B) Differences in the intensity profiles when the AP from the NLMA and the suggested method are applied along the line y = 450

5.5 Comparison using BM-3D

BM-3D is considered a state-of-the-art image-denoising algorithm. Alkinani et al., (2017) have developed their work with the dimensional strong breaking step. Table 5 related the BM-3D PS-NR values, adaptive hard brink BM-3D and the suggested method on "Lena imagery". The outputs are also shown in Fig 8, dimensional hard brink BM-3D has the best PS-NR values at noise levels from ten to thirty and noise levels from sixty to eighty, during BM-3D has the best PS-NR values at noise levels forty and fifty. The suggested method has the best PS-NR values at noise levels over eighty.

Table 5 – PS-NR work of BM-3D, adaptive BM-3D, and the suggested method on Lena imagery

Noise level	10	20	30	40	50	60	70	80	90	100
BM3D	35.87	33.01	31.24	**29.93**	**28.80**	27.71	26.67	25.66	24.70	23.78
Adaptive BM3D	**35.94**	**33.08**	**31.03**	29.92	28.77	**27.73**	**26.73**	**25.75**	24.81	23.91
Proposed method	35.79	32.68	30.63	29.15	27.98	27.07	26.31	25.62	**24.96**	**24.35**

p-ISSN : 1979-0414 e-ISSN : 2621-6256

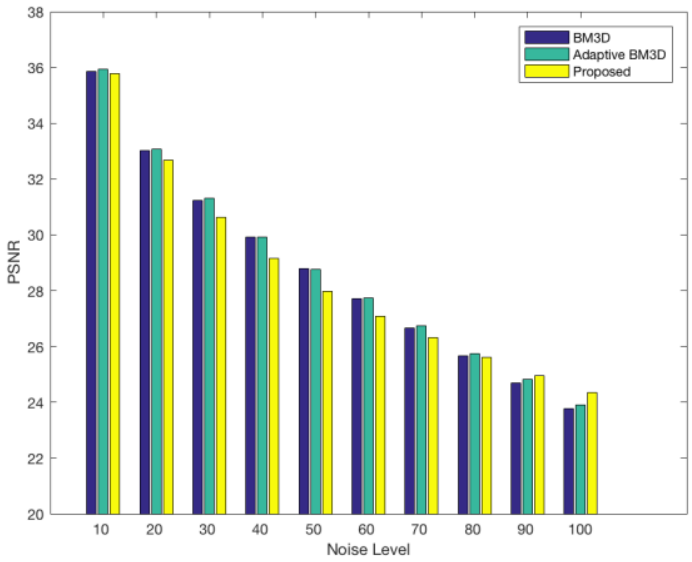

Figure 8 – PS-NR work of BM-3D, adaptive BM-3D, and the suggested method on Lena imagery

6. CONCLUSION

The suggested method surpasses other NLM methods in terms of PS-NR in noise levels over twenty. In the MSS-IM, it has the best outcome when the noise level is no more than seventy. The visual identification shows that the suggested method better preserves edges and textures in images, especially at high noise levels. In the intensity profile, the proposed method mostly has fewer changes to the original image values than the other methods. The WAVRA is important progress across the patch-based noise-canceling algorithms. In this research, the proposed WAV reprojection algorithm method has been refined. The improved methods proposed here include A better analysis design entrenched on the eigenvalues of the tensor matrix structure. It analyzes image pixels into 3 areas: smoothness, edges, and texture/noise. Textures are given plainly at a low noise level, during the noise and textures are granted at a high noise level. Another is, An APS defined as a different pixel entrenched in that pixel class. Several trials are given to choose the best PS for different classes. And last is, the analysis results are also taken as a mask on the noise image to boost the class of identical patches. Only patches whose center pixels are of the same class grant to the averaging process. The suggested mechanism has been related to the NLMA and its several variations in terms of PS-NR and MSS-IM. The results show that the suggested method in this research has been a good choice over another competitive method.

Future Research

The method suggested in this study can be further continued to hue images (color picture). The analysis can even be upgraded because the brightness and chrominance values will be used rather than just grayscale values. Developing the analysis will boost the denoising conduct. The method suggested in this study can also be tested on various kinds of data, such as medical images.

REFERENCES

Amit Kumar Naik, Guddu Kumar, Prabhat Kumar Upadhyay, Paresh Date, & Abhinoy Kumar Singh. (2022). Gaussian Filtering for Simultaneously Occurring Delayed and Missing Measurements. IEEE Access, 10, 100746–100762. https://doi.org/10.1109/ACCESS.2022.3208119

Asif Khan and Mahmoud R El-Sakka. (2016). Non-local means using adaptive weight thresholding. In VISIGRAPP (3: VISAPP), pages 69–78, 2016.

Charles-Alban Deledalle, Vincent Duval, and Joseph Salmon. (2012). Non-local methods with shape-adaptive patches (nlm-sap). Journal of Mathematical Imaging and Vision, 43(2):103–120, 2012.

David L Donoho and Mark R Duncan. (2000). Digital curvelet transform: strategy, implementation, and experiments. In International Society for Optics and Photonics in: Wavelet Applications VII, volume 4056, pages 12–31, 2000.

Dinesh Peter and R Ramya. (2012). A non-local adaptive novel means for image denoising. Procedia Engineering, (38):3278–3282, 2012.

Enders A Robinson and Sven Treitel. (1976). Principles of digital wiener filtering. Geophysical Prospecting, 15(3):311–332, 1967.

Hanan AR Akkar, Wael AH Hadi, & Ibraheem H. Al-Dosari. (2019). A Squared-Chebyshev wavelet thresholding based on 1D signal compression. Defense Technology, 15(3), 426–431. https://doi.org/10.1016/j.dt.2018.08.009

Hans Knutsson. Representing local structures using tensors. In 6th Scandinavian Conference on Image Analysis, pages 244–251, 1989.

Hostettler, R., & Särkkä, S. (2019). Rao-Blackwellized Gaussian Smoothing. https://aaltodoc.aalto.fi/handle/123456789/36223

IJ Umoh, G. Onuh, TH Sikiru, & D. Siman. (2020). An Infrared Image Enhancement Technique Based on Neighborhood Wavelet Thresholding Coefficient for Multi-level Discrete Wavelet Transform. Applications of Modeling and Simulation, 4, 202–209. https://doaj.org/article/38a1636e7b61447897df409c9d3ff49d

Javier Portilla, Vasily Strela, Martin Wainwright, and Eero Simoncelli. (2003). Image denoising using scale mixtures of Gaussians in the wavelet domain. IEEE Transactions in image processing, 12(11), 2003.

Jing Hu and Yu-pin Luo. (2013). Non-local optical means algorithm with adaptive patch size and bandwidth. Optics - International Journal for Light and Electron Optics, 124(22):5639–5645, 2013.

Jingzhong Li, Pengcheng Liu, Wenhao Yu, & Xiaoqiang Cheng. (2018). The morphing of geographical features by Fourier transformation. PLoS ONE, 13(1), 0191136. https://doi.org/10.1371/journal.pone.0191136

Jinhua Lin, Lin Ma, & Jingxia Cui. (2020). A Frequency-Domain Convolutional Neural Network Architecture Based on the Frequency-Domain Randomized Offset Rectified Linear Unit and Frequency-Domain Chunk Max Pooling Method. IEEE Access, 8, 98126–98155. https://doi.org/10.1109/ACCESS.2020.2996250

João, A., Gambaruto, A., & Sequeira, A. (2020). Anisotropic Gradient based Filtering for Object Segmentation in Medical Images. João, A, Gambaruto, A & Sequeira, A 2020, 'Anisotropic Gradient Based Filtering for Object Segmentation in Medical Images', Computer Methods in Biomechanics and Biomedical Engineering: Imaging & Visualization. Https://Doi.Org/10.1080/21681163.2020.1776642 . http://hdl.handle.net/1983/a29f50b8-07b1-4ae4-aa84-eb1f9e5eab6d

Joseph Salmon and Yann Strozecki. (2012). Patch reprojections for non-local methods. Signal Processing, 92(2):477–489, 2012.

Ju-Long Deng. (1982). Control problems of gray systems. Systems and Control Letters, 1(5):288–294, 1982.

Kaizhi Wu, Xuming Zhang, and Mingyue Ding. (2014). Curvelet-based nonlocal means algorithm for image denoising. AEU-International Journal of Electronics and Communications, 68(1):37–43, 2014.

Leonid Rudin and Stanley Osher. Total variation-based image restoration with free local constraints. In IEEE 1st International Conference in Image Processing, volume 1, pages 31–35, 1994.

Mahmud Hasan, & Mahmoud R. El-Sakka. (2018). Improved BM3D image denoising using SSIM-optimized Wiener filter. EURASIP Journal on Image and Video Processing, 2018(1), 1–12. https://doi.org/10.1186/s13640-018-0264-z

May, A. (2022). The Design and Simulation of a Fifth-order Chebyshev Low-Pass Filter. Journal of Physics: Conference Series, 2386(1), 012066. https://doi.org/10.1088/1742-6596/2386/1/012066

Mingju Chen and Pingxian Yang. (2013). An adaptive non-local means image denoising model. In IEEE 2013 6th International Congress on Image and Signal Processing (CISP), volume 1, pages 245–249, 2013.

Mohammed Ghazal and Aishy Amer. (2011). Homogeneity localization using particle filters with applications to noise estimation. IEEE Transactions on image processing, 20(7):1788–1796, 2011.
Monagi Alkinani and Mahmoud El-Sakka. (2017). A modified block matching 3d algorithm for additive noise reduction. Mathematics for Application, (5):93–103, 2017.
Neelam Kumari , PJ (2017). Design Of FIR Low Pass Filter Using Particle Swarm Optimization Algorithm. ISSN:2456-9992. http://www.ijarp.org/published-research-papers/sep2017/Design-Of-Fir-Low-Pass-Filter-Using-Particle-Swarm-Optimization-Algorithm.pdf _
Nijia Qian, Guobin Chang, Jingxiang Gao, Wenbin Shen, & Zhengwen Yan. (2022). Adaptive DDK Filter for GRACE Time-Variable Gravity Field with a Novel Anisotropic Filtering Strength Metric. Remote Sensing, 14(3114), 3114. https://doi.org/10.3390/rs14133114
Othman, G., & Zeebaree, DQ (2020). The Applications of Discrete Wavelet Transform in Image Processing: A Review. Journal of Soft Computing and Data Mining; Vol. 1 No. 2 (2020); 31-43; 2716-621X. http://penerbit.uthm.edu.my/ojs/index.php/jscdm/article/view/7215
Punam Saha and Jayaram Udupa. (2000). New optimum thresholding method using region homogeneity and class uncertainty. In International Society for Optics and Photonics. Medical Imaging: Image Processing, volume 3979, pages 180–192, 2000.
Rajiv Verma and Rajoo Pandey. (2018). Gray relational analysis based adaptive smoothing parameter for non-local means image denoising. Multimedia Tools and Applications, pages 1–22, 2018.
Shujin Zhu, Yuehua Li, and Yuanjiang Li. (2014). Two-stage non-local means filtering with adaptive smoothing parameters. Optics-International Journal for Light and Electron Optics, 125(23):7040–7044, 2014.
Vincent Duval, Jean-Fran¸cois Aujol, and Yann Gousseau. (2011). A bias-variance approach for the NLM algorithm. SIAM Journal on Imaging Sciences, 4(2):760–788, 2011.
Weili Zeng, Yijun Du, and Changhui Hu. (2017). Noise suppression by discontinuity indicator controlled non-local means method. Multimedia Tools and Applications, 76(11):13239–13253, 2017.
WL Zeng and XB Lu. (2011). Region-based non-local means algorithm for noise removal. Electronics Letters, 47(20):1125–1127, 2011.
Xia Lan, Huanfeng Shen, and Liangpei Zhang. (2013). An adaptive non-local means filter based on region homogeneity. In IEEE Seventh International Conference on Image and Graphics, pages 50–54, 2013.
Xinhao Liu, Masayuki Tanaka, and Masatoshi Okutomi. (2012). Noise level estimation using weak textured patches of a single noisy image. In 19th IEEE International Conference on Image Processing (ICIP), pages 665–668, 2012.
Xinhao Liu, Masayuki Tanaka, and Masatoshi Okutomi. (2013). Single-image noise level estimation for blind denoising. IEEE transactions on image processing, 22(12):5226–5237, 2013.
Xu, X., & Zhao, J. (2020). Quaternion Mahalanobis Non-Local Means for Color Image Denoising. Journal of Physics: Conference Series, 1621(1), 012046. https://doi.org/10.1088/1742-6596/1621/1/012046
Yakut, S. (2021). Random Number Generator Based on Discrete Cosine Transform Based Lossy Picture Compression. https://hdl.handle.net/20.500.12899/804